

# Oxidation of $[\text{Ru}(\text{NH}_3)_5\text{isn}](\text{BF}_4)_2$ by Hypochlorous Acid and Chlorine in Aqueous Acidic Media

Basudeb Saha and David M. Stanbury\*

Department of Chemistry, Auburn University, Auburn, Alabama 36849

Received October 2, 2000

UV-vis stopped-flow studies of the reaction of  $[\text{Ru}(\text{NH}_3)_5\text{isn}]^{2+}$  (isn = isonicotinamide) with excess HOCl at 25 °C demonstrate that it proceeds in two time-resolved steps. In the first step  $[\text{Ru}(\text{NH}_3)_5\text{isn}]^{3+}$  is produced with the rate law  $-\text{d}[\text{Ru}(\text{II})]/\text{d}t = 2(aK_h[\text{H}^+] + b[\text{H}^+][\text{Cl}^-] + c[\text{Cl}^-])[\text{HOCl}]_{\text{tot}}[\text{Ru}(\text{II})]/(K_h + [\text{H}^+][\text{Cl}^-])$ . Here,  $K_h$  is  $1.3 \times 10^{-3} \text{ M}^2$  and corresponds to the equilibrium hydrolysis of  $\text{Cl}_2$ ,  $a$  is  $(8.34 \pm 0.19) \times 10^3 \text{ M}^{-2} \text{ s}^{-1}$  and represents the acid-assisted reduction of HOCl,  $b$  is  $(4.04 \pm 0.13) \times 10^4 \text{ M}^{-1} \text{ s}^{-1}$  and represents the reduction of  $\text{Cl}_2$ , and  $c$  is  $(6.25 \pm 0.59) \times 10^2 \text{ s}^{-1}$  and represents the  $\text{Cl}^-$ -assisted reduction of HOCl. In the second step  $[\text{Ru}(\text{NH}_3)_5\text{isn}]^{3+}$  undergoes further oxidation to a mixture of products with the rate law  $-\text{d}[\text{Ru}(\text{III})]/\text{d}t = e[\text{Ru}(\text{III})][\text{HOCl}]/[\text{H}^+]$  where  $e$  is  $(1.18 \pm 0.01) \times 10^{-2} \text{ s}^{-1}$ . This step is assigned a mechanism with  $\text{Cl}^+$  transfer from HOCl to  $[\text{Ru}^{\text{III}}(\text{NH}_3)_4(\text{NH}_2)\text{isn}]^{2+}$  occurring in the rate-limiting step. These results underline the resistance of HOCl to act as a simple outer-sphere one-electron oxidant.

## Introduction

Hypochlorous acid (HOCl) is well-known as a strong oxidant in aqueous solution, and there have been many studies of the kinetics of its reactions. Reports on the kinetics of its reactions with one-electron reductants are much more limited. Studies on the reactions of HOCl with such classic reductants as  $\text{e}^-(\text{aq})$ ,  $\text{H}(\text{aq})$ , and  $\text{CO}_2^-$  appear to be lacking. Its reaction with  $\text{O}_2^-$  is remarkably slow ( $k = 7.5 \times 10^6 \text{ M}^{-1} \text{ s}^{-1}$ )<sup>1</sup> and generates OH radicals.<sup>2</sup> As reviewed by Thompson, reactions of HOCl with a number of metal aquo ion reductants have been studied; the majority of these reactions have inner-sphere mechanisms, and none of them have been demonstrated to proceed by an outer-sphere mechanism.<sup>3</sup> Of the very few studies of potentially outer-sphere reductants, the reaction with  $[\text{Fe}(\text{phen})_3]^{2+}$  is notable in that dissociation of phenanthroline from the Fe(II) complex is one of the rate-limiting steps.<sup>4</sup> A parallel pathway that is first order in  $[\text{HOCl}]$  is also reported to occur with  $k = 2.2 \times 10^{-2} \text{ M}^{-1} \text{ s}^{-1}$ .<sup>4</sup> The reaction with  $[\text{Fe}(\text{CN})_6]^{4-}$  is enigmatic, yielding highly discordant results in its several studies.<sup>5–9</sup> Copper catalysis is the likely cause of these disagreements.<sup>8</sup> The net one-electron oxidation of  $[\text{Ni}(\text{CN})_4]^{2-}$  by HOCl has been argued to proceed with a two-electron rate-determining step.<sup>10</sup> In our own studies of the reactions of aqueous chlorine with  $[\text{Ru}(\text{bpy})_2(\text{NH}_3)_2]^{2+}$ ,  $[\text{Ru}(\text{terpy})_2]^{2+}$ , and related species we found rate laws dominated by reaction of  $\text{Cl}_2$  with no evidence for HOCl-dependent terms.<sup>11,12</sup> These later studies were conducted in

acidic media with high concentrations of chloride to minimize the hydrolysis of  $\text{Cl}_2$  and hence did not provide stringent tests for a minor HOCl pathway. In the present work we describe the reaction of HOCl with  $[\text{Ru}(\text{NH}_3)_5\text{isn}]^{2+}$  (isn = isonicotinamide) under chloride-free conditions. These new results demonstrate the extreme kinetic inertness of HOCl toward reaction with outer-sphere reductants, and they reveal two novel processes: the one-electron reduction of  $\text{H}_2\text{OCl}^+$  and the chloride-assisted one-electron reduction of HOCl.

## Experimental Section

**Reagents and Solutions.** Distilled deionized water was obtained by passing deionized water through a Barnstead pretreatment cartridge and subsequent distillation in a Barnstead Fi-stream all-glass still. Trifluoromethanesulfonic acid ( $\text{CF}_3\text{SO}_3\text{H}$ ) was purchased from 3M, and lithium trifluoromethanesulfonate ( $\text{LiCF}_3\text{SO}_3$ ) was prepared by neutralization of concentrated  $\text{CF}_3\text{SO}_3\text{H}$  with  $\text{Li}_2\text{CO}_3$  (Aldrich). This solution was heated to boiling in order to remove any dissolved  $\text{CO}_2$  gas and allowed to cool to room temperature, whereupon a solid crystalline salt precipitated. Sodium triflate was similarly prepared from  $\text{CF}_3\text{SO}_3\text{H}$  and  $\text{Na}_2\text{CO}_3$ . The concentration of  $\text{CF}_3\text{SO}_3\text{H}$  was determined by titration with standardized NaOH. Chloride-free solutions of hypochlorous acid were prepared according to the method developed by Cady.<sup>13</sup> According to this method, chlorine monoxide was first prepared by the reaction of yellow mercuric oxide with high-purity chlorine gas (Matheson) dissolved in  $\text{CCl}_4$ , and HOCl was obtained by extracting the  $\text{Cl}_2\text{O}$  solution with cold water. This solution was assayed at 254 nm ( $\epsilon_{254} = 59 \text{ M}^{-1} \text{ cm}^{-1}$ ),<sup>11,14</sup> stored in a refrigerator, and used within 2 weeks. Hexaammineruthenium(III) chloride (Alfa), isonicotinamide (Aldrich) (isn),  $\text{NaHSO}_3$  (Fisher),  $\text{H}_2\text{O}_2$  (30%, Fisher),  $\text{NaN}_2$  (MCB),  $\text{HBF}_4$  (Fisher), and  $\text{Na}_2\text{S}_2\text{O}_8$  (Sigma) were used without purification.  $\text{D}_2\text{O}$ , 99.9 atom % D, was purchased from Aldrich.

All solutions were prepared in deionized distilled water. To prevent autoxidation, Ru(II) solutions were prepared by dissolving solid  $[\text{Ru}(\text{NH}_3)_5\text{isn}](\text{BF}_4)_2$  in a bubbling flask containing argon-degassed water. For stopped-flow experiments, requisite volumes of stock  $\text{CF}_3\text{SO}_3\text{H}$ ,  $\text{LiCF}_3\text{SO}_3$ , and  $\text{LiCl}$  solutions were transferred to bubbling flasks and sparged with argon gas. Appropriate volumes of stock HOCl or

- (1) Long, C. A.; Bielski, B. H. J. *J. Phys. Chem.* **1980**, *84*, 555–557.
- (2) Candeias, L. P.; Patel, K. B.; Stratford, M. R. L.; Wardman, P. *FEBS Lett.* **1995**, *333*, 151–153.
- (3) Thompson, R. C. *Adv. Inorg. Bioinorg. Mech.* **1986**, *4*, 65–106.
- (4) Ondrus, M. G.; Gordon, G. *Inorg. Chem.* **1971**, *10*, 474–477.
- (5) Kozlov, Y. N.; Vorob'eva, T. P.; Purmal, A. P. *Russ. J. Phys. Chem.* **1981**, *55*, 1294–1297.
- (6) Lee, H.-F. *J. Chem. Soc., Dalton Trans.* **1988**, 273–275.
- (7) Candeias, L. P.; Stratford, M. R. L.; Wardman, P. *Free Radical Res.* **1994**, *20*, 241–249.
- (8) Prütz, W. A. *Arch. Biochem. Biophys.* **1996**, *332*, 110–120.
- (9) Prütz, W. A. *Monatsh. Chem.* **1997**, *128*, 737–748.
- (10) Beach, M. W.; Margerum, D. W. *Inorg. Chem.* **1990**, *29*, 1225–1232.
- (11) Assefa, Z.; Stanbury, D. M. *J. Am. Chem. Soc.* **1997**, *119*, 521–530.
- (12) Saha, B.; Stanbury, D. M. *Inorg. Chem.* **2000**, *39*, 1294–1300.

- (13) Cady, G. H. *Inorg. Synth.* **1957**, *5*, 156–165.
- (14) Zimmerman, G.; Strong, F. C. *J. Am. Chem. Soc.* **1957**, *79*, 2063–2066.

degassed  $[\text{Ru}(\text{NH}_3)_5\text{isn}]^{2+}$  solution were added to the degassed solutions in the bubbling flasks, and the mixed solutions were immediately transferred by airtight glass syringes. The concentration of the HOCl reactant solution was determined spectrophotometrically for each experiment. For reactions in the HP 8453 spectrophotometer, solutions were prepared directly in a quartz cell (1 cm path length) by adding appropriate volumes of  $\text{CF}_3\text{SO}_3\text{H}$ ,  $\text{LiCF}_3\text{SO}_3$ , water, complex solution, and finally HOCl.

DOCl was prepared by vigorous shaking of a mixture of  $\text{D}_2\text{O}$  and a cold solution of chlorine(I) oxide in carbon tetrachloride in a separatory funnel. The carbon tetrachloride phase was withdrawn, leaving the aqueous layer containing DOCl.

**Preparation of Ruthenium Complexes.** All the ruthenium complexes shown below were prepared starting from  $[\text{Ru}(\text{NH}_3)_5\text{Cl}]\text{Cl}_2$  as described previously.<sup>15</sup>

**$[\text{Ru}(\text{NH}_3)_5\text{isn}](\text{BF}_4)_2$ .** Gaunder's method<sup>16</sup> for the perchlorate salt as described by Stanbury et al.<sup>15</sup> was modified by the use of a saturated solution of sodium tetrafluoroborate to precipitate the  $\text{BF}_4^-$  salt of the complex. It was recrystallized by cooling a warm aqueous solution of the salt, washed with ethanol and ether, and dried in a vacuum desiccator. The compound was characterized by UV-vis and  $^1\text{H}$  NMR spectra. Reported values<sup>17,18</sup> of the molar absorptivity of aqueous solutions of this complex agree with our measured value,  $1.04 \times 10^4 \text{ M}^{-1} \text{ cm}^{-1}$ , at 480 nm.  $^1\text{H}$  NMR ( $\text{D}_2\text{O}$ ,  $\delta$  vs DSS): 8.63 (2H, d) and 7.56 (2H, d). Anal. Calcd for  $[\text{Ru}(\text{NH}_3)_5\text{isn}](\text{BF}_4)_2$ : C, 14.95; H, 4.39; N, 20.34. Found: C, 15.49; H, 4.60; N, 19.59.

**$[\text{Ru}(\text{NH}_3)_5\text{isn}]^{3+}$ .** This compound was prepared following the reported method<sup>15</sup> and obtained as a yellow solid in the form of  $[\text{Ru}(\text{NH}_3)_5\text{isn}]\text{Cl}_3$  with good yield.  $[\text{Ru}(\text{NH}_3)_5\text{isn}](\text{CF}_3\text{SO}_3)_3$  was obtained by metathesis of the chloride salt with very low yield. The molar absorptivity of the chloride salt in 0.01 M  $\text{CF}_3\text{SO}_3\text{H}$  ( $\epsilon_{277} = 6.0 \times 10^3 \text{ M}^{-1} \text{ cm}^{-1}$ ) supports<sup>16</sup> the purity of the compound.

***trans*- $[\text{Ru}(\text{NH}_3)_4(\text{SO}_4)\text{isn}]\text{Cl}$ .** This compound was prepared by adopting the literature procedure.<sup>19,20</sup> *trans*- $[\text{Ru}(\text{NH}_3)_4(\text{SO}_2)\text{Cl}]\text{Cl}_2$  (0.1 g, 0.328 mmol) was dissolved in 1.5 mL of argon-degassed water in a 10 mL bubbling flask, and then a 10-fold excess of isonicotinamide (0.4 g, 3.28 mmol) was added. As the isonicotinamide reacted with  $[\text{Ru}(\text{NH}_3)_4(\text{SO}_2)\text{Cl}]\text{Cl}_2$ , a deep orange color developed and the solution gradually became clear. Following this, 1 mL of 6 M HCl and 2.5 mL of 30%  $\text{H}_2\text{O}_2$  were added immediately into the reaction mixture, resulting in a yellow solution. Addition of excess acetone (20 mL) into the yellow solution produced a yellow precipitate. The solid was filtered off, washed with acetone, and dried under vacuum. The yield was 97% compared to approximately 83% as reported by earlier authors.

***trans*- $[\text{Ru}(\text{NH}_3)_4(\text{NO})\text{isn}](\text{BF}_4)_3$ .** This complex was prepared from *trans*- $[\text{Ru}(\text{NH}_3)_4(\text{SO}_4)\text{isn}]\text{Cl}$  according to the reported<sup>19,22</sup> method and characterized by  $^1\text{H}$  NMR, IR, and UV-vis spectra. Yield: 64%.  $^1\text{H}$  NMR ( $\text{D}_2\text{O}$ ,  $\delta$  vs DSS): 8.71 (2H, d) and 8.23 (2H, d). Infrared data ( $\text{cm}^{-1}$ ): 3400 [ $\nu(\text{NH}_2)$  and  $\nu(\text{NH}_3)$ , w], 3208 [ $\nu(\text{NH}_3)$ , s], 1934 [ $\nu(\text{NO})$ , s], 1695 [amide I, s], 1622 [amide II and  $\text{NH}_2$  deformation, m], 1354 [ $\nu(\text{ring})$ , m], 1085 [ $\nu(\text{BF}_4)$ , s], 861 [C-H (deformation) out of plane, w], 738, 611 [ $\nu(\text{Ru}-\text{NO})$ , m] and 496 [ $\nu(\text{Ru}-\text{NH}_3)$ , w]. UV-vis aqueous molar absorptivities ( $\text{M}^{-1} \text{ cm}^{-1}$ ):  $1.16 \times 10^4$  (230 nm, peak),  $3.48 \times 10^3$  (268 nm, shoulder),  $2.33 \times 10^2$  (323 nm) and 26 (486 nm). The value at 268 nm is significantly higher than reported by Gomes et al.,<sup>19</sup> but the others are very close to the literature values.

**Methods.** UV-vis spectra were recorded on a HP-8453 diode array spectrophotometer equipped with a thermostated water bath to maintain the temperature at  $25.0 \pm 0.1$  °C. A Corning pH meter, model 130, with a Mettler semimicro combination glass electrode was used for pH measurements. The glass electrode was calibrated using an analytically prepared solution of known  $[\text{H}^+]$  to obtain actual concentrations of hydrogen ion from measured pH values. Cyclic voltammograms (CV) and Osteryoung square-wave voltammograms (OSWV) were recorded with 0.1 M  $\text{NaClO}_4$  as supporting electrolyte using a BAS-100 electrochemical analyzer employing a conventional three-electrode cell with a glassy carbon working electrode, a platinum wire auxiliary electrode, and a Ag/AgCl reference electrode. Some experiments were also conducted using a gold working electrode. Potential values are expressed relative to NHE by adding 0.197 as  $E^\circ$  for the Ag/AgCl electrode. Infrared spectra were recorded on a Bruker Equinox 55 FTIR spectrophotometer.  $^1\text{H}$  NMR spectra were obtained at room temperature with a Bruker AC 250 instrument and 5 mm sample tubes.

The reaction of  $[\text{Ru}(\text{NH}_3)_5\text{isn}]^{2+}$  was studied on a Hi-Tech Scientific model SF-51 stopped-flow apparatus with a SU-40 spectrophotometer unit in the 1.0 cm path length configuration. Temperature was maintained at 25 °C with a C-400 circulatory water bath. Reactions were monitored by mixing equal volumes of the two reactants, both of which were maintained at 0.2 M ionic strength. An OLIS 4300S system was used for data acquisition and analysis. Multiwavelength spectral scans for the reaction between  $[\text{Ru}(\text{NH}_3)_5\text{isn}]^{2+}$  and HOCl were obtained using an OLIS rapid scanning monochromator stopped-flow system (RSM 1000) with the USA-SF mixing attachment (1.7 cm path length). Kinetics measurements of the reaction of  $[\text{Ru}(\text{NH}_3)_5\text{isn}]^{3+}$  were monitored on a HP-8453 spectrophotometer using stoppered 1 cm quartz cuvettes.

## Results

Preliminary study of the aqueous reaction of excess chloride-free HOCl with  $[\text{Ru}(\text{NH}_3)_5\text{isn}]^{2+}$  showed that it proceeds rapidly with the complete consumption of the Ru(II) complex. At low pH the loss of Ru(II) displayed good pseudo-first-order kinetics, but at higher pH (>2.5) the reaction traces showed significant deviations from exponential behavior. Further experiments indicated a complex stoichiometry and mechanism, and thus a detailed investigation of the reaction was conducted.

**UV-Vis Product Spectra.** In a preliminary experiment, a  $1.37 \times 10^{-4}$  M Ru(II) solution was oxidized with HOCl in an approximately 2:1 molar ratio at  $[\text{NaCF}_3\text{SO}_3] = 0.1$  M and pH = 1.5 ( $\text{CF}_3\text{SO}_3\text{H}$ ). The spectrum of the product solution showed a peak at 267 nm. The same experiment in the presence of 0.2 mM  $\text{Cl}^-$  also showed a peak at 267 nm in the product solution. Spectra of the product solutions from another set of experiments done at pH 4.0 under identical conditions showed the peak position somewhat shifted to 262 nm, but the UV-vis spectrum of an aqueous solution of authentic  $[\text{Ru}(\text{NH}_3)_5\text{isn}]^{3+}$  showed the peak at 277 nm. Thus the peak position of the product solution has blue shifted from that of pure  $[\text{Ru}(\text{NH}_3)_5\text{isn}]^{3+}$ . To see this effect in the presence of excess HOCl, 0.1 mM  $[\text{Ru}(\text{NH}_3)_5\text{isn}]^{2+}$  was oxidized with 5 mM HOCl at pH 1.5. Excess HOCl was then converted to  $\text{Cl}_2$  by adding 0.2 M  $\text{Cl}^-$  according to the equilibrium



and then removed by sparging the solution with  $\text{N}_2$  gas. UV-vis spectra of the HOCl-free product solution show a peak at 262 nm, which is again 15 nm lower than for solutions of pure  $[\text{Ru}(\text{NH}_3)_5\text{isn}]^{3+}$ . To check the recovery of starting Ru(II), the pH of this product solution was increased to 3.1 by dropwise addition of NaOH followed by addition of  $\text{Na}_2\text{S}_2\text{O}_3$  to reduce Ru(III) back to Ru(II). Only a 71% recovery of Ru(II) was determined by spectrophotometry at 480 nm. When a similar

- (15) Stanbury, D. M.; Haas, O.; Taube, H. *Inorg. Chem.* **1980**, *19*, 518–524.  
 (16) Gaunder, R. G.; Taube, H. *Inorg. Chem.* **1970**, *9*, 2627–2639.  
 (17) Ford, P.; Rudd, D. F. P.; Gaunder, R.; Taube, H. *J. Am. Chem. Soc.* **1968**, *90*, 1187–1194.  
 (18) Rocha, Z. N.; Chiericato, G.; Tfouni, E. In *Electron-Transfer Reactions*; Isied, S. S., Ed.; American Chemical Society: Washington, DC, 1997; pp 297–313.  
 (19) Gomes, M. G.; Davanzo, C. U.; Silva, S. C.; Lopes, L. G. F.; Santos, P. S.; Franco, D. W. *J. Chem. Soc., Dalton Trans.* **1998**, 601–607.  
 (20) Brown, G. M.; Sutton, J. E.; Taube, H. *J. Am. Chem. Soc.* **1978**, *100*, 2767–2774.  
 (21) Vogt, L. H., Jr.; Katz, J. L.; Wiberly, S. E. *Inorg. Chem.* **1965**, *4*, 1157–1163.  
 (22) Borges, S. S. S.; Davanzo, C. U.; Castellano, E. E.; Z-Schpector, J.; Silva, S. C.; Franco, D. W. *Inorg. Chem.* **1998**, *37*, 2670–2677.

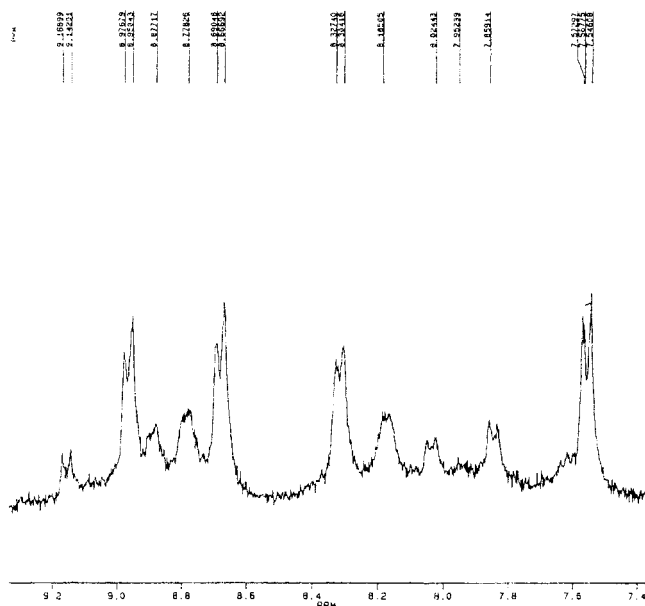


**Figure 1.** Aromatic region of  $^1\text{H}$  NMR spectrum of the product solution from the reaction between  $[\text{Ru}(\text{NH}_3)_5\text{isn}]^{2+}$  and  $\text{DOCl}$  at pH 3.5 after addition of  $\text{Na}_2\text{S}_2\text{O}_3$  to reduce  $\text{Ru}(\text{III})$  species back to  $\text{Ru}(\text{II})$ . Full spectrum shown in Figure S-1.

experiment was performed at pH 4.0, only a 16% recovery of  $\text{Ru}(\text{II})$  was obtained. As we show below, the  $^1\text{H}$  NMR spectra indicate that  $\text{trans-}[\text{Ru}^{\text{II}}(\text{NH}_3)_4(\text{NO})\text{isn}]^{3+}$  is among the product species. Aqueous solutions of this species have a strong absorption in the far UV with a sharp shoulder at 265 nm, features that could account for some of the spectral shifts noted above for the oxidized product mixtures.

**$^1\text{H}$  NMR Product Spectra.** Two experiments were performed to characterize the products by  $^1\text{H}$  NMR spectroscopy. In the first experiment, a concentrated solution of  $[\text{Ru}(\text{NH}_3)_5\text{isn}]^{2+}$  in  $\text{D}_2\text{O}$  was oxidized with excess  $\text{DOCl}$  at pH 1.1, adjusted by one drop of concentrated aqueous  $\text{CF}_3\text{SO}_3\text{H}$ . The  $^1\text{H}$  NMR spectrum of this solution showed no significant peak in the aromatic region. In the second experiment a  $[\text{Ru}(\text{NH}_3)_5\text{isn}]^{2+}$  solution in  $\text{D}_2\text{O}$  was oxidized with  $\text{DOCl}$  at pH 3.5, and the  $^1\text{H}$  NMR spectrum of this solution showed a series of doublets in the aromatic region ( $\delta$  vs DSS) at 8.99, 8.90, 8.7, 8.32, 8.18, and 8.02 ppm. Solid  $\text{Na}_2\text{S}_2\text{O}_3$  was then added to reduce  $\text{Ru}(\text{III})$  back to  $\text{Ru}(\text{II})$ . Small shifts in the above peak positions occurred due to removal of paramagnetic  $\text{Ru}(\text{III})$ , the most significant being a shift of the 8.7 ppm resonance to 8.77 ppm after  $\text{S}_2\text{O}_3^{2-}$  addition. Moreover, four new doublets appeared at 9.16, 8.66, 7.85, and 7.57 ppm (Figures 1 and S-1 (Supporting Information)). Of the four new resonances, two ( $\delta$  8.66 and 7.57) are due to the generation of  $[\text{Ru}(\text{NH}_3)_5\text{isn}]^{2+}$ .<sup>19</sup> Two of the resonances found both prior to  $\text{S}_2\text{O}_3^{2-}$  addition and after (8.7 and 8.18 ppm prior to  $\text{S}_2\text{O}_3^{2-}$  addition, and 8.77 and 8.18 ppm after) are assigned to  $\text{trans-}[\text{Ru}^{\text{II}}(\text{NH}_3)_4(\text{NO})\text{isn}]^{3+}$ .

These results imply that with excess  $\text{HOCl}$  at pH 1.1 the  $\text{Ru}(\text{II})$  is converted completely to a paramagnetic species, while at pH 3.5 a mixture is produced that contains  $[\text{Ru}(\text{NH}_3)_5\text{isn}]^{3+}$ ,  $\text{trans-}[\text{Ru}^{\text{II}}(\text{NH}_3)_4(\text{NO})\text{isn}]^{3+}$ , and other species.

**Stoichiometry.** With  $\text{Ru}(\text{II})$  in excess over hypochlorous acid, stoichiometric experiments were conducted at varying concentrations of both of the reactants adopting the following conditions:  $[\text{Ru}(\text{II})]_0 = 0.2\text{--}0.3$  mM,  $[\text{HOCl}]_0 = 0.05\text{--}0.1$  mM, pH = 1.51,  $[\text{NaCF}_3\text{SO}_3] = 0.1$  M, and temperature 25 °C. Parallel blank experiments with no  $\text{HOCl}$  were also performed to account for any decomposition of  $\text{Ru}(\text{II})$ . Unreacted  $\text{Ru}(\text{II})$  was

**Table 1.** Stoichiometry of the Oxidation of  $[\text{Ru}(\text{NH}_3)_5\text{isn}]^{2+}$  by  $\text{HOCl}^a$

$[\text{Ru}(\text{II})]_0$ , mM	$[\text{HOCl}]_{\text{tot},0}$ , mM	$[\text{Cl}^-]_0$ , mM	$\Delta[\text{Ru}(\text{II})]$ , mM	$\Delta[\text{Ru}(\text{II})]/\Delta[\text{HOCl}]_{\text{tot}}$
0.200	0.100	-	0.164	1.64
0.200	0.0500	-	0.089	1.78
0.300	0.100	-	0.174	1.74
0.200	0.100	0.100	0.166	1.66
0.200	0.0500	0.100	0.100	2.00
0.300	0.100	0.100	0.183	1.83

<sup>a</sup> pH 1.51,  $\mu = 0.1$  M ( $\text{NaCF}_3\text{SO}_3$ ), and temperature 25 °C.  $[\text{HOCl}]_{\text{tot}} = [\text{Cl}_2] + [\text{HOCl}]$ .

measured by spectrophotometry at 480 nm, and the stoichiometric ratios, as shown in Table 1, were calculated from the consumption of  $\text{Ru}(\text{II})$  to the total  $\text{HOCl}$ . Similar experiments were carried out in the presence of 0.2 mM  $\text{Cl}^-$ , and the results are also included in Table 1. The measured consumption ratios ( $\Delta[\text{Ru}(\text{II})]/\Delta[\text{HOCl}]$ ) show no pronounced trends with conditions and have an average value of  $1.78 \pm 0.13$ . Within two standard deviations this result is consistent with a net one-electron oxidation of  $\text{Ru}(\text{II})$  and reduction of  $\text{HOCl}$  to  $\text{Cl}^-$ .

**Electrochemistry.** The cyclic voltammogram of  $[\text{Ru}(\text{NH}_3)_5\text{isn}]^{2+}$  solution at pH 1.7 and  $[\text{NaClO}_4] = 0.1$  M shows a quasi-reversible wave with  $E_{1/2} = 399$  mV vs NHE and  $\Delta E_{p/p} = 78$  mV at a sweep rate of 100 mV/s using a glassy carbon working electrode. Use of a gold working electrode produced  $E_{1/2} = 402$  mV and  $\Delta E_{p/p} = 86$  mV at the sweep rate 50 mV/s. These values are very close to 387 mV<sup>15</sup> reported in 0.1 M  $\text{HCl}$  at a Pt wire working electrode and  $400 \pm 10$  mV as reported by Chou et al.<sup>23</sup> OSWV showed  $E_p = 401$  mV using a glassy carbon working electrode and no evidence for the presence of more than one species in the solution. This  $\text{Ru}(\text{II})$  solution was then oxidized with excess  $\text{HOCl}$ , the excess  $\text{HOCl}$  was converted to  $\text{Cl}_2$  by addition of 0.2 M  $\text{HCl}$ , and the  $\text{Cl}_2$  was then removed by an argon sparge. Cyclic voltammetric analysis of this product solution showed no well-resolved set of waves.

**Kinetics. Consumption of  $[\text{Ru}(\text{NH}_3)_5\text{isn}]^{2+}$  by  $\text{HOCl}$ .** Kinetic studies of this reaction were conducted at 25 °C under pseudo-first-order conditions with  $\text{HOCl}$  in excess over  $[\text{Ru}(\text{NH}_3)_5\text{isn}]^{2+}$ , monitoring the decay of  $\text{Ru}(\text{II})$  at 480 nm on a stopped-flow spectrophotometer. The kinetic conditions adopted are  $[\text{HOCl}] = 1.20\text{--}9.45$  mM,  $[\text{Ru}(\text{II})]_0 = 0.04\text{--}0.05$  mM,  $[\text{H}^+] = 0.013\text{--}0.2$  M, and  $\mu = 0.2$  M ( $\text{LiCF}_3\text{SO}_3$ ). The kinetic traces are monophasic showing good single-exponential behavior, and the  $k_{\text{obs}}$  value is defined by

$$-d[\text{Ru}(\text{II})]/dt = k_{\text{obs}}[\text{Ru}(\text{II})] \quad (2)$$

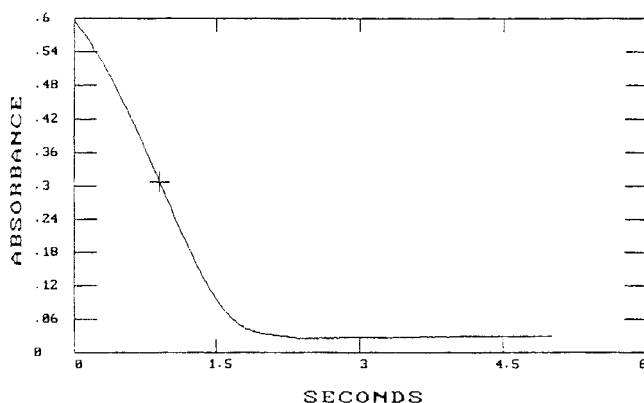
Table 2 shows the dependence of the pseudo-first-order rate constants ( $k_{\text{obs}}$ ,  $\text{s}^{-1}$ ) on  $[\text{HOCl}]$ ,  $[\text{H}^+]$ , and  $[\text{Cl}^-]$ . A plot of  $k_{\text{obs}}$  vs  $[\text{HOCl}]$  in 0.33 M  $\text{H}^+$  under  $\text{Cl}^-$ -free conditions is linear (Figure S-2 (Supporting Information)) with an intercept very close to zero indicating a first-order dependence on  $[\text{HOCl}]$ . The reaction is very sensitive to the acidity of the medium, giving a linear plot of  $k_{\text{obs}}/[\text{HOCl}]$  vs  $[\text{H}^+]$  over the range 0.013–0.18 M  $\text{H}^+$  as shown in Figure S-3 (Supporting Information); this plot has a well-defined slope of  $(1.78 \pm 0.04) \times 10^4$   $\text{M}^{-2} \text{s}^{-1}$ , and the intercept ( $8.76 \pm 36.3$   $\text{M}^{-1} \text{s}^{-1}$ ) is not statistically resolved from zero. The kinetic traces at lower acid concentrations ( $[\text{H}^+] < 0.013$  M) deviate significantly from first-order behavior with an autocatalytic appearance (Figure 2). At these lower acidities the first half-life decreases with an increase

(23) Chou, M. H.; Creutz, C.; Sutin, N. *Inorg. Chem.* **1992**, *31*, 2318–2327.

**Table 2.** Kinetic Dependence of the Oxidation of  $[\text{Ru}(\text{NH}_3)_5\text{isn}]^{2+}$  by HOCl on  $[\text{H}^+]$ ,  $[\text{HOCl}]$ , and  $[\text{Cl}^-]$ <sup>a</sup>

$[\text{H}^+]$ , M	$[\text{HOCl}]_{\text{tot}}$ , mM	$[\text{Cl}^-]_0$ , mM	$k_{\text{obs}}$ , s <sup>-1</sup>	$[\text{H}^+]$ , M	$[\text{HOCl}]_{\text{tot}}$ , mM	$[\text{Cl}^-]_0$ , mM	$k_{\text{obs}}$ , s <sup>-1</sup>
0.033	1.20	0.0	0.64	0.033	5.12	0.1	5.13
0.033	2.83	0.0	1.63	0.033	4.90	0.3	8.07
0.033	5.08	0.0	2.94	0.033	5.12	0.6	14.5
0.033	6.52	0.0	3.25	0.033	5.0	1.0	20.3
0.033	9.45	0.0	5.08	0.033	4.70	0.0	2.86 <sup>b</sup>
0.013	4.75	0.0	1.07	0.049	5.0	1.0	23.2
0.023	4.75	0.0	1.96	0.072	5.0	1.0	29.6
0.049	5.0	0.0	4.91	0.10	5.0	1.0	36.5
0.072	5.42	0.0	6.57	0.135	5.0	1.0	45.8
0.10	5.40	0.0	9.60	0.20	1.0	200	84.8
0.135	5.30	0.0	13.1	0.05	1.0	200	96.6
0.18	5.40	0.0	17.1	0.033	1.0	170	101.0

<sup>a</sup> Other conditions:  $\mu = 0.2$  M ( $\text{LiCF}_3\text{SO}_3$ ),  $[\text{Ru}(\text{NH}_3)_5\text{isn}^{2+}]_0 = 0.04\text{--}0.05$  mM, and 25 °C. Concentration of hypochlorous acid of each experiment was determined spectrophotometrically at 254 nm.  $[\text{HOCl}]_{\text{tot}} = [\text{Cl}_2] + [\text{HOCl}]$ . <sup>b</sup>  $\mu = 0.1$  M ( $\text{LiCF}_3\text{SO}_3$ ).

**Figure 2.** Kinetic trace showing non-pseudo-first-order behavior of reaction between 0.05 mM  $[\text{Ru}(\text{NH}_3)_5\text{isn}]^{2+}$  and 5.29 mM HOCl at pH 4.3,  $[\text{NaOAc}] = 0.02$  M,  $\mu = 0.1$  M ( $\text{NaCF}_3\text{SO}_3$ ), and temperature 25 °C. Monitored at 480 nm.

in pH. As a brief study of the ionic strength dependence, one experiment was performed at  $\mu = 0.1$  M, but no significant difference in rate constant was found (at  $[\text{H}^+] = 0.033$  M,  $\mu = 0.2$  M, and  $[\text{HOCl}] = 5.08$  mM,  $k_{\text{obs}}$  is 2.94 s<sup>-1</sup>; at  $\mu = 0.1$  M and  $[\text{HOCl}] = 4.7$  mM,  $k_{\text{obs}}$  is 2.84 s<sup>-1</sup> under the same acid concentration).

The reaction rate is strongly accelerated by chloride ion (0.1–1.0 mM) at constant  $[\text{H}^+] = 0.033$  M as shown in Table 2. Under these conditions a significant portion of the HOCl is converted to  $\text{Cl}_2$  through reaction 1, and so we report results in terms of total chlorine:

$$[\text{HOCl}]_{\text{tot}} = [\text{HOCl}] + [\text{Cl}_2] \quad (3)$$

The plot of  $k_{\text{obs}}/[\text{HOCl}]_{\text{tot}}$  vs  $[\text{Cl}^-]$  is linear (Figure S-4 (Supporting Information)) with intercept =  $(6.27 \pm 0.55) \times 10^2$  M<sup>-1</sup> s<sup>-1</sup> and slope =  $(3.49 \pm 0.1) \times 10^6$  M<sup>-2</sup> s<sup>-1</sup>. The acceleration is due to the formation of aqueous chlorine in the presence of chloride ion, whose reactivity is higher than that of hypochlorous acid. Acid variation experiments ( $[\text{H}^+] = 0.033\text{--}0.13$  M) at a constant chloride concentration (1.0 mM) show a linear dependence of  $k_{\text{obs}}/[\text{HOCl}]_{\text{tot}}$  on  $[\text{H}^+]$  (Figure S-5 (Supporting Information)), the intercept and slope values being  $(2.15 \pm 0.17) \times 10^3$  M<sup>-1</sup> s<sup>-1</sup> and  $(5.29 \pm 0.2) \times 10^4$  M<sup>-2</sup> s<sup>-1</sup>, respectively. These results at  $[\text{H}^+] \geq 0.013$  M are consistent with rate law 4, which is presented in a form that is compatible with the mechanism proposed in the Discussion below:

$$k_{\text{obs}} = 2(aK_{\text{h}}[\text{H}^+] + b[\text{H}^+][\text{Cl}^-] + c[\text{Cl}^-]) \frac{[\text{HOCl}]_{\text{tot}}}{K_{\text{h}} + [\text{H}^+][\text{Cl}^-]} \quad (4)$$

A nonlinear least-squares fit of eq 4 with all the experimental data (Table 2) provides a good agreement of experimental and calculated values of  $k_{\text{obs}}/[\text{HOCl}]_{\text{tot}}$  for  $K_{\text{h}} = 8.0 \times 10^{-4}$  M<sup>2</sup> at  $\mu = 0.2$  M, interpolated from the data reported by Wang et al.<sup>24</sup> However, optimization of fit was achieved for  $K_{\text{h}} = 1.3 \times 10^{-3}$  M<sup>2</sup>, and the corresponding values of  $a$ ,  $b$ , and  $c$  are  $(8.34 \pm 0.19) \times 10^3$  M<sup>-2</sup> s<sup>-1</sup>,  $(4.04 \pm 0.13) \times 10^4$  M<sup>-1</sup> s<sup>-1</sup>, and  $(6.25 \pm 0.59) \times 10^2$  s<sup>-1</sup> respectively. The mild deviation of  $K_{\text{h}}$  from its literature value may be due to use of a different salt to maintain the ionic strength.

A number of blank experiments were performed. As  $\text{CCl}_4$  is present at low concentrations in the above experiments because of the method of preparation of HOCl, a test was performed to determine if it was responsible for the deviations from pseudo-first-order behavior at high pH. Increasing the  $\text{CCl}_4$  concentration by use of a saturated solution of  $\text{CCl}_4$  led to no significant effect on the kinetic traces. Likewise, addition of PBN, a radical spin trapping agent, had no significant effect. As a test for possible metal ion catalysis and chelating effect, the addition of  $\text{Cu}^{2+}$  (0.1–0.3 mM) and 1,10-phenanthroline (0.1–0.4 mM) had no effect on the kinetics under the conditions of  $[\text{HOCl}] = 5$  mM and pH 1.0. The effect of Ru(III) (added to the reactant Ru(II) solution) was studied under the conditions of  $[\text{Ru(II)}]_0 = 0.05$  mM, pH = 1.58,  $\mu = 0.1$  M ( $\text{NaCF}_3\text{SO}_3$ ). Without Ru(III), the value of  $k_{\text{obs}}$  was 2.5 s<sup>-1</sup> for  $[\text{HOCl}] = 4.8$  mM, and it was apparently unchanged at 2.7 s<sup>-1</sup> with the addition of 0.1 mM Ru(III) for  $[\text{HOCl}] = 4.9$  mM.

It is clear from rate law 4 that the third term becomes dominant at lower acidities for significant concentrations of chloride. It is tempting to suggest that the autocatalysis observed at lower acidities under “chloride-free” conditions is due to the formation of chloride as a product of the reaction as was found for the reaction of HOCl with  $[\text{Fe}(\text{phen})_3]^{2+}$ .<sup>25</sup> However, the behavior under these conditions requires a more complex mechanism in order to explain the observed decrease in first half-lives with increasing pH as described above.

**Kinetics. Reaction of  $[\text{Ru}(\text{NH}_3)_5\text{isn}]^{3+}$  with HOCl.** This reaction was investigated with an excess of HOCl over  $[\text{Ru}(\text{NH}_3)_5\text{isn}]^{3+}$ , with  $[\text{Ru(III)}]_0 = 0.1$  mM,  $[\text{H}^+] = (44.0\text{--}1.51) \times 10^{-3}$  M,  $\mu = 0.2$  M ( $\text{LiCF}_3\text{SO}_3$ ), and temperature 25 °C. It proceeds with an isosbestic point at 273 nm and a loss of absorbance at 277 nm ( $\lambda_{\text{max}}$  for Ru(III)) (Figure 3). These results indicate that the reaction is monophasic and that the Ru(III) is converted to products that also absorb in the UV. 100% conversion of Ru(III) to *trans*- $[\text{Ru}^{\text{II}}(\text{NH}_3)_4(\text{NO})\text{isn}]^{3+}$  would give a final absorbance of 0.32 at 277 nm ( $\epsilon_{277} = 3.23 \times 10^3$  M<sup>-1</sup> cm<sup>-1</sup>), but in fact the final absorbance was 0.48. The low absorbance change may be due to the formation of other species with high molar absorptivity at 277 nm, an interpretation that is consistent with the <sup>1</sup>H NMR results described above. Despite the complexity of the product mixture, the kinetic traces at 277 nm displayed good pseudo-first-order behavior with  $k_{\text{obs}}$  increasing with an increase in pH as shown in Table 3. For solutions less acidic than those reported in Table 3 the kinetic traces are more complex, showing an increase in absorbance that occurs after the initial decay. The data in Table 3 at 5 mM  $\text{H}^+$  yield a linear plot of  $k_{\text{obs}}$  vs  $[\text{HOCl}]$  (Figure S-6 (Supporting Informa-

(24) Wang, T. X.; Margerum, D. W. *Inorg. Chem.* **1994**, *33*, 1050–1055.(25) Shakhshiri, B. Z.; Gordon, G. *Inorg. Chem.* **1968**, *7*, 2454–2456.

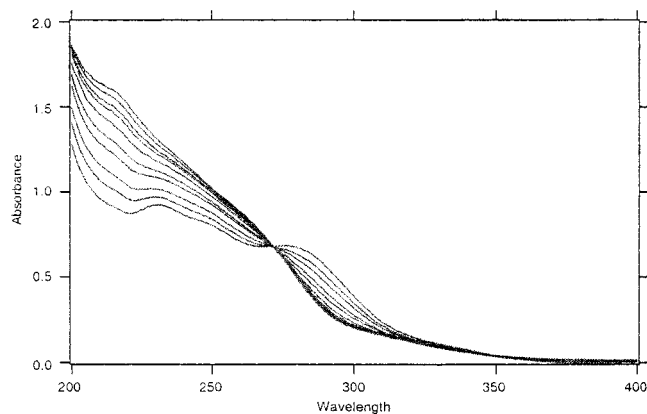


**Figure 3.** Spectral profile of the reaction of  $[\text{Ru}(\text{NH}_3)_5\text{isn}]^{3+}$  and HOCl at  $[\text{Ru}(\text{NH}_3)_5\text{isn}^{3+}]_0 = 0.1$  mM,  $[\text{HOCl}] = 5$  mM,  $[\text{H}^+] = 0.019$  M,  $\mu = 0.2$  M ( $\text{LiCF}_3\text{SO}_3$ ), and temperature  $25$  °C. Original data were collected in 20 s intervals, for a total of 1000 s, and are shown in 100 s intervals.

**Table 3.** Kinetic Dependence of the Reaction between  $[\text{Ru}(\text{NH}_3)_5\text{isn}]^{3+}$  and HOCl on  $[\text{H}^+]$  and  $[\text{HOCl}]^a$

$[\text{H}^+]$ , mM	$[\text{HOCl}]$ , mM	$10^3 k_{\text{obs}}$ , $\text{s}^{-1}$	$k_{\text{obs}}/[\text{HOCl}]$ , $\text{M}^{-1} \text{s}^{-1}$
5.0	2.0	7.36	3.68
5.0	5.0	19.1	3.82
5.0	0.5	1.88	3.76
5.0	0.8	3.19	3.98
5.0	1.0	3.25	3.25
5.0	3.75	14.1	3.75
44.0	5.0	1.67	0.33
19.0	5.0	3.90	0.78
6.45	5.0	12.1	2.42
3.80	1.0	4.39	4.39
1.82	1.0	6.90	6.90
1.51	5.0	40.5	8.10

<sup>a</sup> Other conditions:  $[\text{Ru}(\text{NH}_3)_5\text{isn}^{3+}]_0 = 0.1$  mM,  $\mu = 0.2$  M ( $\text{LiCF}_3\text{SO}_3$ ), and  $25$  °C.  $k_{\text{obs}}$  values were obtained from the first-order exponential fitting of the decay curve.  $[\text{H}^+]$  was calculated from measured pH of the solution using a calibrated electrode.

tion) with an intercept very close to zero indicating a first-order dependence on  $[\text{HOCl}]$ .

Values of  $k_{\text{obs}}/[\text{HOCl}]$  increase approximately linearly with  $[\text{H}^+]^{-1}$  as shown in Figure S-7 (Supporting Information), although there is some suggestion of saturation behavior at high  $[\text{H}^+]^{-1}$ . Attempts to resolve the behavior at higher pH were unsuccessful because under these conditions the kinetic traces become biphasic, showing a rise in absorbance after the initial decay. A linear fit of the data in Figure S-7 yields an intercept of  $0.61 \pm 0.35 \text{ M}^{-1} \text{ s}^{-1}$  and a slope ( $e$ ) of  $(1.18 \pm 0.01) \times 10^{-2} \text{ s}^{-1}$ . Thus, the general rate law, considering high uncertainty in the intercept, may be represented by

$$-d[\text{Ru(III)}]/dt = e[\text{Ru(III)}][\text{HOCl}]/[\text{H}^+] \quad (5)$$

**Overall Kinetics of Ru(II) Oxidation.** The above results suggest that the reaction of  $[\text{Ru}(\text{NH}_3)_5\text{isn}]^{2+}$  with excess HOCl proceeds in two time-resolved steps. The first is the formation of  $[\text{Ru}(\text{NH}_3)_5\text{isn}]^{3+}$ , while the second is the further oxidation of  $[\text{Ru}(\text{NH}_3)_5\text{isn}]^{3+}$ . This sequence was confirmed by an experiment monitored at 277 nm with  $[\text{H}^+] = 0.033$  M,  $[\text{Ru(II)}]_0 = 0.035$  mM,  $[\text{HOCl}] = 4.5$  mM, and  $\mu = 0.2$  M ( $\text{LiCF}_3\text{SO}_3$ ). Dual-time reaction traces were taken with 100 data points in 1 s followed by 100 points in the next 1500 s, as is shown in Figure 4. The initial rapid increase in absorbance is a clear indication of the formation of  $[\text{Ru}(\text{NH}_3)_5\text{isn}]^{3+}$  in the first step,

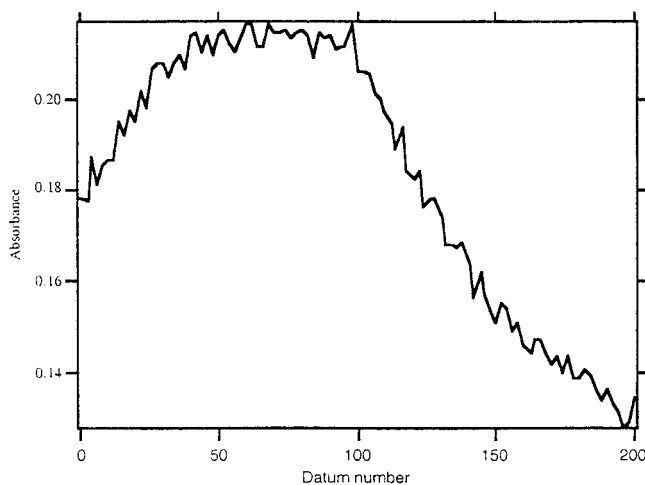


**Figure 4.** Dual-time trace at 277 nm for the reaction between  $[\text{Ru}(\text{NH}_3)_5\text{isn}]^{2+}$  and HOCl at  $[\text{Ru}(\text{NH}_3)_5\text{isn}^{2+}]_0 = 0.035$  mM,  $[\text{HOCl}] = 4.5$  mM,  $\mu = 0.2$  M ( $\text{LiCF}_3\text{SO}_3$ ),  $[\text{H}^+] = 0.033$  M, and temperature  $25$  °C. Initial 100 points show the formation of  $[\text{Ru}(\text{NH}_3)_5\text{isn}]^{3+}$  in 1 s, and the next 100 points show the decay of  $[\text{Ru}(\text{NH}_3)_5\text{isn}]^{3+}$  in 1500 s.

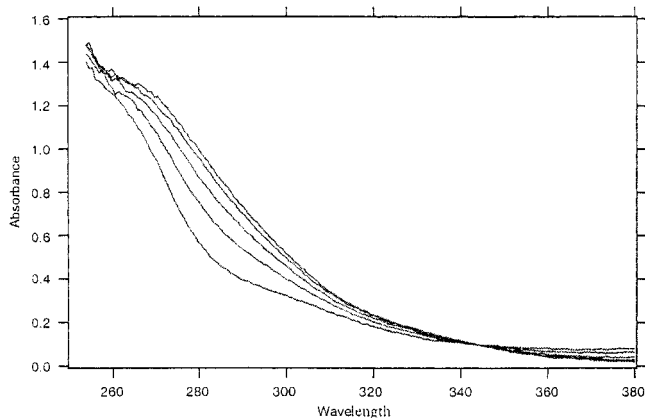


**Figure 5.** OLIS rapid-scan spectra showing the formation of Ru(III) (at 277 nm) in the first step of the reaction between  $[\text{Ru}(\text{NH}_3)_5\text{isn}]^{2+}$  and hypochlorous acid at  $[\text{Ru(II)}]_0 = 0.05$  mM,  $[\text{HOCl}]_{\text{tot},0} = 4.0$  mM,  $[\text{H}^+] = 0.033$  M,  $\mu = 0.2$  M ( $\text{LiCF}_3\text{SO}_3$ ), and temperature  $25$  °C. Original data were collected in 16 ms intervals and are shown in 320 ms intervals.

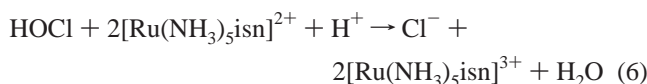
while the slower absorbance decrease corresponds to the second step. Rapid-scan spectra of this reaction show an absorbance increase at 277 nm, which also supports the formation of  $[\text{Ru}(\text{NH}_3)_5\text{isn}]^{3+}$  in the first step (Figure 5). The  $c$  term of the rate law is predominant at  $[\text{H}^+] = 0.01$  M and  $[\text{Cl}^-] = 0.2$  M, and the rapid-scan spectral behavior under these conditions reveals formation of the same species (Figure S-8 (Supporting Information)) as obtained when the  $a$  term is dominant. Note that Figure S-8 differs from Figure 5 in the region near 325 nm because of the absorption arising from  $\text{Cl}_2$  in the former.

Since the first step decreases in rate as the pH increases, while the opposite trend occurs for the second step, the kinetics of the reaction of Ru(II) at higher pH occurs on the same time scale as the further oxidation of Ru(III). We suggest that the oxidation of Ru(III) generates an intermediate that can consume Ru(II), thus contributing to the kinetic complexities observed in the oxidation of Ru(II) at higher pH.

## Discussion

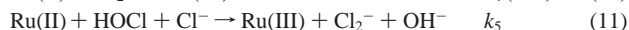
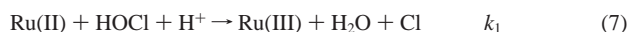
The general features of the reaction of HOCl with  $[\text{Ru}(\text{NH}_3)_5\text{isn}]^{2+}$  depend on the composition of the solutions. With excess Ru(II) the consumption ratios are consistent with a simple

stoichiometry:



With excess HOCl at higher pH the NMR data indicate formation of a complex mixture of products, one of which has been identified as *trans*-[Ru<sup>II</sup>(NH<sub>3</sub>)<sub>4</sub>(NO)isn]<sup>3+</sup>. The complexity of the product mixture is revealed by the large number of resonances in the <sup>1</sup>H NMR, the lack of a well-resolved CV, and the nature of its UV spectrum. On the other hand, the biphasic kinetics observed in the UV implies that simple oxidation of [Ru(NH<sub>3</sub>)<sub>5</sub>isn]<sup>2+</sup> occurs in the rapid initial phase, while the second phase corresponds to the further oxidation of [Ru(NH<sub>3</sub>)<sub>5</sub>isn]<sup>3+</sup> to *trans*-[Ru<sup>II</sup>(NH<sub>3</sub>)<sub>4</sub>(NO)isn]<sup>3+</sup> and other products.

**Mechanism of [Ru(NH<sub>3</sub>)<sub>5</sub>isn]<sup>2+</sup> Oxidation.** A plausible mechanism for the oxidation of [Ru(NH<sub>3</sub>)<sub>5</sub>isn]<sup>2+</sup> in the rapid step is given by reactions 1 and 7–11.



If the steady-state approximation is made for [Cl] and [Cl<sub>2</sub><sup>-</sup>], the derived rate law is

$$-d[\text{Ru(II)}]/dt = 2(k_1[\text{HOCl}][\text{H}^+] + k_3[\text{Cl}_2] + k_5[\text{HOCl}][\text{Cl}^-])[\text{Ru(II)}] \quad (12)$$

Interconversion between Cl and Cl<sub>2</sub><sup>-</sup> through the well-known reaction



is also a likely component of the mechanism, but its occurrence does not affect eq 12. Use of the equilibrium hydrolysis of Cl<sub>2</sub> as in reaction 1 provides eqs 14 and 15:

$$[\text{HOCl}] = \frac{[\text{HOCl}]_{\text{tot}}K_h}{K_h + [\text{H}^+][\text{Cl}^-]} \quad (14)$$

$$[\text{Cl}_2] = \frac{[\text{HOCl}]_{\text{tot}}[\text{H}^+][\text{Cl}^-]}{K_h + [\text{H}^+][\text{Cl}^-]} \quad (15)$$

The overall rate law, eq 12, can be rewritten as

$$-\frac{d[\text{Ru(II)}]}{dt} = 2(k_1K_h[\text{H}^+] + k_3[\text{H}^+][\text{Cl}^-] + k_5K_h[\text{Cl}^-])\frac{[\text{HOCl}]_{\text{tot}}[\text{Ru(II)}]}{K_h + [\text{H}^+][\text{Cl}^-]} \quad (16)$$

Equation 16 is equivalent to the observed rate law 4, where *a*, *b*, and *c* are *k*<sub>1</sub>, *k*<sub>3</sub>, and *k*<sub>5</sub>*K*<sub>h</sub>, respectively.

The first term in the rate law corresponds to the acid-assisted reduction of HOCl by Ru(II) (reaction 7). Use of NBS data<sup>26</sup> for appropriate Δ<sub>r</sub>G° values (neglecting the hydration free energy

for Cl(g)) plus *E*° for the Ru(III)/Ru(II) couple leads to a calculated value for Δ<sub>r</sub>G° of -90 kJ mol<sup>-1</sup> for reaction 7, which is a clear indication of the plausibility of this step in the mechanism. A detailed mechanism for this process (*k*<sub>1</sub>) entails the formation of hypochlorous acidium ion, H<sub>2</sub>OCl<sup>+</sup>, in a prior equilibrium step according to



One-electron reduction of H<sub>2</sub>OCl<sup>+</sup> would lead to the indicated products. Although such a one-electron reaction has no literature precedent in HOCl chemistry, formation of this highly reactive chlorine species in acidic media has been reported by several authors.<sup>27–30</sup> Two possible positively charged chlorine species are H<sub>2</sub>OCl<sup>+</sup> and Cl<sup>+</sup>, and thermodynamic arguments show that Cl<sup>+</sup> should be highly unstable relative to H<sub>2</sub>OCl<sup>+</sup>.<sup>31</sup> The higher chlorination rates of benzene, toluene, and sodium α-toluene-sulfonate with hypochlorous acid in the presence of sulfuric and perchloric acid have been interpreted by the formation of H<sub>2</sub>OCl<sup>+</sup>.<sup>28</sup> The same author in the earlier communication also showed that H<sub>2</sub>OCl<sup>+</sup> reacts in the first step without waiting for the formation of chlorinium ions, Cl<sup>+</sup>.<sup>32</sup> The final word demolishing Cl<sup>+</sup> as an intermediate was published by Swain et al.,<sup>30</sup> who were able to refute a prior claim for rate-limiting Cl<sup>+</sup> formation in the acid-dependent chlorination of anisole by hypochlorous acid; in this same paper they presented evidence for the formation of H<sub>2</sub>OCl<sup>+</sup> in a prior equilibrium step, though they were unable to rule out the termolecular alternative. Derbyshire et al.<sup>29</sup> reported an approximate value of 10<sup>-4</sup> M<sup>-1</sup> for *K*. If we assume that this is a correct value, then from *k*<sub>1</sub> we can calculate the actual reactivity of H<sub>2</sub>OCl<sup>+</sup> with Ru(II) as 8 × 10<sup>7</sup> M<sup>-1</sup> s<sup>-1</sup>.

Rate constant *k*<sub>3</sub> represents the reactivity of Cl<sub>2</sub> with Ru(II), and its value is (4.04 ± 0.13) × 10<sup>4</sup> M<sup>-1</sup> s<sup>-1</sup>. An outer-sphere electron-transfer mechanism is reasonably assigned for this step in view of the kinetic inertness of Ru(II) and the identity of the Ru(III) product. Outer-sphere reduction of Cl<sub>2</sub> by [Ru(bpy)<sub>2</sub>(NH<sub>3</sub>)<sub>2</sub>]<sup>2+</sup>, [Ru(terpy)<sub>2</sub>]<sup>2+</sup>, and related species has also been reported.<sup>11,12</sup> Evidence that all these reactions have outer-sphere mechanisms is presented in Figure 6, which demonstrates an inverse relationship between log *k*<sub>3</sub> - (1/2)log *k*<sub>22</sub> and *E*°-(reductant) where *k*<sub>22</sub> is the self-exchange rate constant for the pertinent metal complex reductant. According to the cross relationship of Marcus theory, such an inverse relationship is to be expected for a series of related outer-sphere reactions. Outer-sphere mechanisms have been well established for reactions between pentaammineruthenium(II) complexes with other diatomic oxidants, e.g., O<sub>2</sub>,<sup>15</sup> I<sub>2</sub>,<sup>33</sup> and Br<sub>2</sub>,<sup>34</sup> and reasonable estimates have been made of the effective self-exchange rate constants for the X<sub>2</sub>/X<sub>2</sub><sup>-</sup> couples. Such estimates require an accurate value for the X<sub>2</sub>/X<sub>2</sub><sup>-</sup> reduction potential, which unfortunately is lacking for the Cl<sub>2</sub>/Cl<sub>2</sub><sup>-</sup> redox couple. Estimates of this *E*° value range from 0.43 to 0.7 V,<sup>35</sup> although we have recently assigned a lower limit of 0.54 V.<sup>12</sup> If the reduction

(27) de la Mare, P. D. B.; Bolton, R. *Electrophilic Additions to Unsaturated Systems*, 2nd ed.; Elsevier: New York, 1982; pp 97–99.

(28) de la Mare, P. D. B.; Harvey, J. T.; Hassan, M.; Varma, S. *J. Chem. Soc.* **1958**, 2756–2759.

(29) Derbyshire, D. H.; Waters, W. A. *J. Chem. Soc.* **1951**, 73–75.

(30) Swain, C. G.; Crist, D. R. *J. Am. Chem. Soc.* **1972**, *94*, 3195–3200.

(31) Bell, R. P.; Gelles, E. *J. Chem. Soc.* **1951**, 2734–2740.

(32) de la Mare, P. D. B.; Ketley, A. D.; Vernon, C. A. *J. Chem. Soc.* **1954**, 1290–1297.

(33) Sun, J.; Stanbury, D. M. *Inorg. Chem.* **1998**, *37*, 1257–1263.

(34) Plotkin, S.; Haim, A. *Inorg. Chim. Acta* **1998**, *270*, 189–196.

(35) Stanbury, D. M. *Adv. Inorg. Chem.* **1989**, *33*, 69–138.

(26) Wagman, D. D.; Evans, W. H.; Parker, V. B.; Schumm, R. H.; Halow, I.; Bailey, S. M.; Churney, K. L.; Nuttall, R. L. *J. Phys. Chem. Ref. Data* **1982**, *11*, Suppl. No. 2.

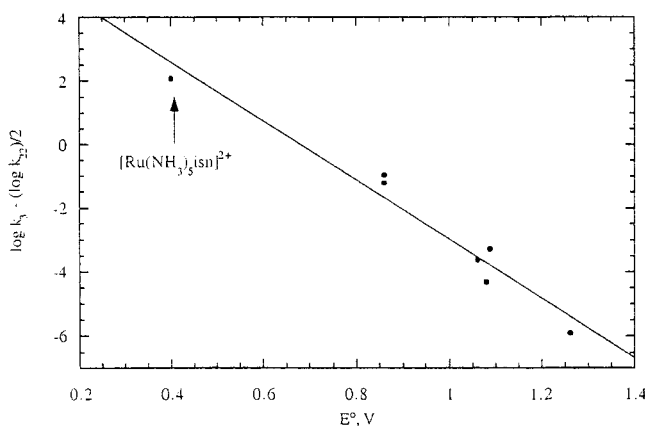


**Figure 6.** Plot of  $\log k_3 - (\log k_{22})/2$  vs  $E^\circ$  for a series of outer-sphere reductants.  $k_{22}$  is the self-exchange rate constant for the reductant. Data from Table S-1 (Supporting Information). Points correspond to oxidations of  $[\text{Ru}(\text{terpy})_2]^{2+}$ ,  $[\text{Ru}(4,7\text{-Me}_2\text{phen})_3]^{2+}$ ,  $[\text{Ru}(4,4'\text{-Me}_2\text{-bpy})_3]^{2+}$ ,  $[\text{Fe}(\text{phen})_3]^{2+}$ ,  $[\text{Fe}(3,4,7,8\text{-Me}_4\text{phen})_3]^{2+}$ ,  $[\text{Ru}(\text{bpy})_2(\text{NH}_3)_2]^{2+}$ , and  $[\text{Ru}(\text{NH}_3)_5\text{isn}]^{2+}$ . The solid line is the result of a linear least-squares fit (slope =  $-9.3$ ).

potential is indeed this high or higher, the lower rate constant for oxidation of  $[\text{Ru}(\text{NH}_3)_5\text{isn}]^{2+}$  by  $\text{Cl}_2$  than by  $\text{Br}_2$  ( $E^\circ = 0.58$  V)<sup>34</sup> implies that the  $\text{Cl}_2/\text{Cl}_2^-$  self-exchange rate constant is significantly smaller than for  $\text{Br}_2/\text{Br}_2^-$ . This inference is supported by theoretical calculations that predict a substantially greater inner-sphere reorganization energy for the  $\text{Cl}_2/\text{Cl}_2^-$  redox couple.<sup>36</sup>

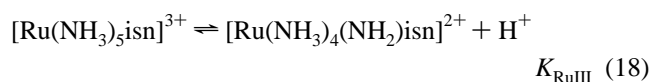
The composite parameter,  $k_5K_h$ , is attributed to the chloride-assisted reaction of  $[\text{Ru}(\text{NH}_3)_5\text{isn}]^{2+}$  with HOCl, as shown by reaction 11. Although such a pathway is unprecedented in HOCl chemistry, we are unaware of any prior studies that were conducted under conditions appropriate to reveal it. An explanation of the assistance lies in the stabilization of the products through formation of nascent  $\text{Cl}_2^-$ : the corresponding transition-state stabilization is suggested by the magnitude of the equilibrium constant for reaction 13,  $1.4 \times 10^5 \text{ M}^{-1}$ .<sup>37</sup> An alternative interpretation of this term is that it arises from the reaction of  $\text{Cl}_2$  with  $[\text{Ru}(\text{NH}_3)_4(\text{NH}_2)\text{isn}]^+$  ( $k_{\text{am}}$ ), in which case parameter  $c$  corresponds to  $k_{\text{am}}K_{\text{Ru}}$  where  $K_{\text{Ru}}$  is the acid dissociation constant for  $[\text{Ru}(\text{NH}_3)_5\text{isn}]^{2+}$ . From the reported  $\text{p}K_{\text{a}}$  value of 10.5 for  $[\text{Ru}(\text{NH}_3)_5\text{isn}]^{3+}$ ,<sup>23</sup> one can reasonably estimate that  $\text{p}K_{\text{Ru}}$  for  $[\text{Ru}(\text{NH}_3)_5\text{isn}]^{2+}$  must be greater than 10.5. In combination with the experimental  $c$  value, this estimate of  $K_{\text{Ru}}$  for  $[\text{Ru}(\text{NH}_3)_5\text{isn}]^{2+}$  leads to a lower limit of  $2.0 \times 10^{13} \text{ M}^{-1} \text{ s}^{-1}$  for  $k_{\text{am}}$ , which is well beyond the limit of diffusion control. Thus we are able to rule out this alternative interpretation. Further evidence against this alternative is that the reaction (Figure 5) yields  $[\text{Ru}(\text{NH}_3)_5\text{isn}]^{3+}$ , while reaction via  $\text{Cl}_2$  with  $[\text{Ru}(\text{NH}_3)_4(\text{NH}_2)\text{isn}]^+$  would be expected to yield an oxidized amine ligand as was found for the oxidation of  $[\text{Ru}(\text{bpy})_2(\text{NH}_3)(\text{NH}_2)]^{2+}$  by chlorine.<sup>11</sup>

Notably absent from the various paths in the mechanism is the direct bimolecular reduction of HOCl by Ru(II). Optimal conditions to detect such a path would be provided by experiments with chloride-free solutions at high pH. However, under these conditions the reaction displays autocatalytic kinetics. By performing experiments under similar conditions, Ondrus and Gordon identified the occurrence of such a pathway

in the reaction of HOCl with  $[\text{Fe}(\text{phen})_3]^{2+}$ .<sup>4</sup> Autocatalysis was a complication in that study as well, and therefore the rate law was determined by the method of initial rates. We have elected not to perform kinetic fits with data showing autocatalytic character, which may explain why we have not detected the bimolecular pathway in the Ru(II) reaction. Nevertheless, it is clear that the bimolecular one-electron reduction of HOCl is not readily identified. Current estimates indicate a value of 0.25 V for the HOCl/HOCl<sup>-</sup> reduction potential,<sup>35</sup> which would make simple electron transfer from Ru(II) to HOCl an endothermic process. This barrier makes it understandable why alternative redox pathways are so prevalent in HOCl chemistry.

**Mechanism of Reaction between  $[\text{Ru}(\text{NH}_3)_5\text{isn}]^{3+}$  and HOCl.** A mechanism of the reaction of  $[\text{Ru}(\text{NH}_3)_5\text{isn}]^{3+}$  with HOCl consistent with the observed rate law (eq 5) is presented in Scheme 1.

### Scheme 1



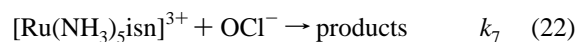
Thus the rate law corresponding to above scheme is

$$-\frac{d[\text{Ru(III)}]}{dt} = \frac{k_6 K_{\text{RuIII}}}{[\text{H}^+]} [\text{Ru}(\text{NH}_3)_5\text{isn}^{3+}] [\text{HOCl}]_{\text{tot}} \quad (20)$$

Comparing eq 20 with general rate eq 5, we have  $e = k_6 K_{\text{RuIII}} = (1.18 \pm 0.01) \times 10^{-2} \text{ s}^{-1}$ . Chou et al.<sup>23</sup> have estimated the  $\text{p}K_{\text{a}}$  value in reaction 18 to be 10.5 from the electrochemical behavior of Ru(II) at high pH. With this estimate for the  $K_{\text{RuIII}}$  value, the bimolecular rate constant corresponding to the deprotonated Ru(III) species,  $k_6$ , is  $(3.73 \pm 0.03) \times 10^8 \text{ M}^{-1} \text{ s}^{-1}$ .

An alternate possible mechanism of the reaction of  $[\text{Ru}(\text{NH}_3)_5\text{isn}]^{3+}$  with HOCl is shown in Scheme 2.

### Scheme 2



The rate law derived from Scheme 2 is given in eq 23.

$$-\frac{d[\text{Ru(III)}]}{dt} = \frac{k_7 K_{\text{HOCl}}}{[\text{H}^+]} [\text{Ru}(\text{NH}_3)_5\text{isn}^{3+}] [\text{HOCl}] \quad (23)$$

Comparison of eqs 23 and 5 makes the following identity:  $e = k_7 K_{\text{HOCl}} = (1.18 \pm 0.01) \times 10^{-2} \text{ s}^{-1}$ . The well-known proton dissociation equilibrium constant of hypochlorous acid,  $K_{\text{HOCl}}$  ( $3.2 \times 10^{-8} \text{ M}$ ),<sup>38</sup> provides a value of  $(3.69 \pm 0.03) \times 10^5 \text{ M}^{-1} \text{ s}^{-1}$  for  $k_7$ .

We favor Scheme 1 for the following reasons. Scheme 2 would imply outer-sphere formation of  $\text{OCl}^{2-}$  or H-atom abstraction to form HOCl<sup>-</sup>, both of which seem unlikely in view of the reactivity already discussed for Ru(II). Scheme 1, on the other hand, could easily proceed through formal  $\text{Cl}^+$  transfer

(36) Stanbury, D. M. In *Electron-Transfer Reactions*; Isied, S., Ed.; American Chemical Society: Washington, DC, 1997; pp 165–182.

(37) Buxton, G. V.; Rydder, M.; Salmon, G. A. *J. Chem. Soc., Faraday Trans.* **1998**, *94*, 653–657.

(38) Smith, R. M.; Martell, A. E.; Motekaitis, R. J. *NIST Critically Selected Stability Constants of Metal Complexes Database, 4.0*; U.S. Department of Commerce: Gaithersburg, MD, 1997.

to the coordinated amide, as has been proposed in the chlorination of free ammonia, alkylamines, and *cis*-[Ru(bpy)<sub>2</sub>(NH<sub>3</sub>)<sub>2</sub>]<sup>3+</sup>.<sup>11,39</sup> Margerum et al. have reported that nucleophilic attack of amines on HOCl (Cl<sup>+</sup> transfer) occurs with rate constants in the range 10<sup>6</sup>–10<sup>8</sup> M<sup>-1</sup> s<sup>-1</sup> and that the rate constants increase with the basicity of the amines.<sup>39</sup> We find that the value of *k*<sub>6</sub> derived from Scheme 1 correlates very well with the trend reported by Margerum et al., provided that we consider 1/*K*<sub>RuIII</sub> to represent the basicity of an amine.

In our prior study of the reaction of *cis*-[Ru(bpy)<sub>2</sub>(NH<sub>3</sub>)<sub>2</sub>]<sup>3+</sup> with HOCl/Cl<sub>2</sub> we found clean conversion to the corresponding nitrosyl derivative and spectroscopic evidence for the formation of an intermediate in what is clearly a multistep process.<sup>11</sup> In the present study a product mixture is obtained, one component of which has been identified as the nitrosyl derivative. Although the other components have not been identified, it is evident that they must be produced after the rate-limiting step for consumption of [Ru(NH<sub>3</sub>)<sub>5</sub>isn]<sup>3+</sup>. By analogy with the reaction of *cis*-[Ru(bpy)<sub>2</sub>(NH<sub>3</sub>)<sub>2</sub>]<sup>3+</sup>, at least one intermediate must be formed along the path to the nitrosyl derivative. Presumably, in the case of the reaction of [Ru(NH<sub>3</sub>)<sub>5</sub>isn]<sup>3+</sup> this intermediate can lead to a mixture of products.

## Conclusions

The reaction of [Ru(NH<sub>3</sub>)<sub>5</sub>isn]<sup>2+</sup> with HOCl proceeds in two time-resolved steps, the first of which yields [Ru(NH<sub>3</sub>)<sub>5</sub>isn]<sup>3+</sup> while the second leads to higher oxidation products. The first step has three terms in the rate law: (1) bimolecular oxidation by H<sub>2</sub>OCl<sup>+</sup>, (2) bimolecular oxidation by Cl<sub>2</sub>, and (3) Cl<sup>-</sup>-assisted oxidation by HOCl. The second step corresponds to Cl<sup>+</sup> transfer from HOCl to the amide ligand of [Ru<sup>III</sup>(NH<sub>3</sub>)(NH<sub>2</sub>)isn]<sup>2+</sup>. These results underline the resistance of HOCl to act as a simple outer-sphere oxidant, and they demonstrate the variety of alternative pathways that can intervene in attempts to enforce such a mechanism.

**Acknowledgment.** This research was supported by a grant from the NSF.

**Supporting Information Available:** Table S-1 and Figures S-1 through S-8. This material is available free of charge via the Internet at <http://pubs.acs.org>.

IC0010914

(39) Margerum, D. W.; Gray, E. T., Jr.; Huffman, R. P. In *Organometals and Organometalloids*; Brinckman, F. E., and Bellama, J. M., Eds.; American Chemical Society: Washington, DC, 1978; pp 278–291.